Journal of Organometallic Chemistry 880 (2019) 232–240

Contents lists available at ScienceDirect

Journal of Organometallic Chemistry

journal homepage: www.elsevier.com/locate/jorganchem

N-methylation versus oxidative addition using MeI in the reaction of organoplatinum(II) complexes containing pyrazine ligand

Niroomand Hosseini Fatemeh [a, *], Zahra Farasat [b], S. Masoud Nabavizadeh [b, c, **], Guang Wu [c], Mahdi M. Abu-Omar [c, ***]

[a] Department of Chemistry, Shiraz Branch, Islamic Azad University, Shiraz, 71993–37635, Iran
[b] Professor Rashidi Laboratory of Organometallic Chemistry, Department of Chemistry, College of Sciences, Shiraz University, Shiraz, 71467-13565, Iran
[c] Department of Chemistry and Biochemistry, University of California, Santa Barbara, CA, 93106, United States

ARTICLE INFO

Article history:
Received 15 August 2018
Received in revised form
31 October 2018
Accepted 1 November 2018
Available online 3 November 2018

This article is dedicated to Professor Richard J. Puddephatt, a pioneer of organplatinum chemistry, on the occasion of his 75th birthday.

Keywords:
Platinum
N-methylation
Oxidative addition
DFT calculation
Kinetic and mechanism

ABSTRACT

The new cyclometalated platinum(II) complexes [PtMe(C^N)(pyrazine)] [C^N = benzo[h]quinolate (bhq), **1a**; C^N = 2-phenylpyridinate (ppy), **1c**] have been prepared by the reaction of corresponding dimethylsulfide complexes with pyrazine. These complexes contain two potential nucleophilic centers, Pt(II) center and free N atom of pyrazine which can compete in the reaction with methyl iodide to give Pt(IV) oxidative addition or N-methylation products, respectively. To investigate which center is more reactive toward MeI, DFT calculations (based on the free energy barrier needed for N-methylation versus oxidative addition reactions) and experimental evidence is considered to predict and explain site selectivity. Both experimental and theoretical studies show that the oxidative addition of MeI to cyclometalated Pt(II) complexes occurs readily to give the Pt(IV) complexes. Theoretical results support remarkably the kinetic results obtained through UV–Vis spectroscopy which suggest an S_N2 mechanism.

1. Introduction

N-methylated compounds are important intermediates in the chemical industry and their functionality is found in medicines, dyes, and perfumes [1,2]. Currently, formaldehyde is used in industrial N-methylations, whereas methyl iodide and dimethylsulphates are usually used on a small scale [3,4]. Recently, Beller et al. and Leitner et al. reported ruthenium-based catalysts for the N-methylation of amines using CO_2 and H_2 as sources of methyl group [5,6]. Shi et al. also described a new heterogeneous catalyst for the preparation of N-methylated compounds from amines, nitriles, and nitro compounds [7]. Therefore, the study of efficient methylation processes has attracted great attention.

On the other hand, oxidative addition of MeI to square-planar d^8 complexes is of special interest because of its significant application in catalysis, an example being the Monsanto process for acetic acid production [8]. It is shown that the oxidative addition of alkyl halides to these complexes proceeds through an S_N2 mechanism which was first suggested on the basis of the kinetic order and the similarity of the activation parameters, for reaction of *trans*-[IrCl(CO)$(PPh_3)_2$] (Vaska's compound) with MeI to those for the Menschutkin reaction [9]. Kinetic isotope effect study involving the reaction of CH_3I/CD_3I with some organotransition metal complexes has also been reported to confirm the operation of the S_N2 mechanism in the oxidative addition of MeI to Vaska's compound and some organoplatinum(II) complexes [10–13].

Among the square-planar d^8 species, organoplatinum(II) complexes of formula [PtMe(C^N)(L)], where C^N is a chelating carbon-nitrogen donor ligand such as 2-phenylpyridinate (ppy) or benzo[h]quinolate (bhq) and L is a phosphorous donor ligand, are the most reactive substrates for oxidative addition reactions [14–19].

* Corresponding author.
** Corresponding author. Professor Rashidi Laboratory of Organometallic Chemistry, Department of Chemistry, College of Sciences, Shiraz University, Shiraz, 71467-13565, Iran.
*** Corresponding author.
E-mail addresses: niroomand@iaushiraz.ac.ir, fniroomand55@yahoo.com (N.H. Fatemeh), nabavizadeh@shirazu.ac.ir (S.M. Nabavizadeh), abuomar@chem.ucsb.edu (M.M. Abu-Omar).

https://doi.org/10.1016/j.jorganchem.2018.11.002
0022-328X/

In this work, we extend our work on a competition between two essential reactions, oxidative addition versus N-methylation [20]. We here report the preparation of two new cyclometalated platinum complexes of the type [PtMe(C^N)(pz)], pz = pyrazine. Pyrazine binds to Pt(II) to form organoplatinum complexes in which a noncoordinated nitrogen atom of the pyrazine ring can behave as a potential site for electrophilic reactions. On the other hand, there will be a competition between Pt(II) center and the free nitrogen of pyrazine for methylation with MeI. To understand which one, Pt(II) or the free N atom of pyrazine is the stronger nucleophile, we studied the mechanism of MeI addition to cycloplatinated(II) complexes. The reactions of cyclometalated platinum(II) complexes having pyridine (py) as ligand, where only oxidative addition reactions are possible, were investigated to provide a reference point.

2. Experimental section

2.1. General remarks

^{1}H NMR spectra were recorded on a Varian 500 or 600 MHz spectrometer in $CDCl_3$ as solvent and referenced to external TMS (0.00 ppm). All chemical shifts and coupling constants are given in ppm and Hz, respectively. The microanalyses for pyridine complexes were performed using a Thermofnigan Flash EA-1112 CHNSO rapid elemental analyzer. In the case of pyrazine complexes, excess pyrazine was difficult to remove, so no elemental analysis was reported. Melting points were recorded on a Buchi 530 apparatus. UV–vis spectra and kinetics were recorded on a PerkinElmer Lambda 25 spectrophotometer with temperature control using an EYELA NCB-3100 constant-temperature bath. [PtMe(bhq)(SMe_2)], **A**, and [PtMe(ppy)(SMe_2)], **B**, were prepared as reported previously [21].

2.2. Synthesis of Pt complexes

[PtMe(bhq)(pz)], **1a**. To an NMR solution of [PtMe(bhq)(SMe_2)], **A**, (10 mg in 1 mL $CDCl_3$) was added in excess of pyrazine (40 mg) at room temperature and the mixture was stirred for 2 h. Product **1a** was formed and characterized by ^{1}H NMR spectroscopy: δ 1.12 [s, 3H, $^2J_{PtH}$ = 87.6 Hz, Me ligand], 7.30 [m, 1H, CH group adjacent to coordinated C atom]; 7.49–8.76 [10H, protons of C^N and pz ligands], 8.94 [m, 1H, $^3J_{PtH}$ = 15.9 Hz, CH group adjacent to coordinated N atom].

[PtMe(bhq)(py)], **1b**. Pyridine (10 μL) was added to a solution of [PtMe(ppy)(SMe_2)], **A**, (50 mg) in acetone (20 mL). The mixture was stirred at room temperature for 1 h. After removal of the solvent by evaporation, a residue was obtained which was further purified by repeated washing with diethyl ether. The product was dried under vacuum. Yield: 88%, mp = 167 °C (decomp). Anal. Calcd. for $C_{19}H_{16}N_2Pt$: C, 48.8; H, 3.5; N, 6.0; Found: C, 48.6; H, 3.3; N, 5.9.^{1}H NMR data: δ 1.19 [s, 3H, $^2J_{PtH}$ = 85.4 Hz, Me ligand], 7.34 [m, 1H, CH group adjacent to coordinated C atom]; 7.51–8.27 [11H, protons of C^N and py ligand], 9.00 [m, 1H, $^3J_{PtH}$ = 15.9 Hz, CH group adjacent to coordinated N atom].

The following complexes were prepared similarly using complex **B** and pyridine or pyrazine.

[PtMe(ppy)(pz)], **1c**. ^{1}H NMR data: δ 0.92 [s, 3H, $^2J_{PtH}$ = 84.5 Hz, Me ligand], 6.97 [m, 1H, CH group adjacent to coordinated C atom]; 7.02–8.75 [10H, protons of C^N and pz ligand], 8.84 [m, 1H, $^3J_{PtH}$ = 15.2 Hz CH group adjacent to coordinated N atom].

[PtMe(ppy)(py)], **1d**. Yield: 84%, mp = 159 °C (decomp). Anal. Calcd. for $C_{17}H_{16}N_2Pt$: C, 46.0; H, 3.6; N, 6.3; Found: C, 45.8; H, 3.4; N, 6.1.^{1}H NMR data: δ 0.96 [s, 3H, $^2J_{PtH}$ = 83.4 Hz, Me ligand], 6.69 [m, 1H, CH group adjacent to coordinated C atom]; 7.04–7.90 [11H, protons of C^N and py ligand], 8.88 [m, 1H, $^3J_{PtH}$ = 15.7 Hz, CH group adjacent to coordinated N atom].

[$PtMe_2$I(bhq)(pz)], **2a**. MeI (10 μL) was added to a solution of **1a** (prepared by addition of 40 mg pyrazine to 10 mg of complex **A** in 1 mL $CDCl_3$) at room temperature. The reaction mixture was stirred for 1 h, and then ^{1}H NMR was recorded: δ 1.20 [s, 3H, $^2J_{PtH}$ = 73.5 Hz, Me ligand *trans* to N atom of C^N ligand]; 1.84 [s, 3H, $^2J_{PtH}$ = 69.5 Hz, Me ligand *trans* to I], 7.50–8.45 [11H, protons of C^N and pz ligand], 10.35 [m, 1H, $^3J_{PtH}$ = 8.8 Hz, CH group adjacent to coordinated N atom].

[$PtMe_2$I(bhq)(py)], **2b**. An excess of MeI (100 μL) was added to a solution of complex **1b**, (40 mg) in 25 mL of acetone at room temperature. The mixture was allowed to stand at this condition for 1 h, and then the solvent was removed under reduced pressure. The residue was washed twice with ether, and the product was dried under vacuum. Yield: 78%, mp = 197 °C (decomp). Anal. Calcd. for $C_{20}H_{19}IN_2Pt$: C, 39.4; H, 3.1; N, 4.6; Found: C, 39.5; H, 3.3; N, 4.5.^{1}H NMR data: δ 1.20 [s, 3H, $^2J_{PtH}$ = 70.4 Hz, Me ligand *trans* to N atom of C^N ligand], 1.95 [s, 3H, $^2J_{PtH}$ = 69.4 Hz, Me ligand *trans* to I], 7.02 [m, 1H, CH group adjacent to coordinated C atom], 7.54–8.63 [11H, protons of C^N and py ligand], 10.13 [m, 1H, $^3J_{PtH}$ = 10.8 Hz, CH group adjacent to coordinated N atom].

The following complexes were prepared similarly using the appropriate Pt complex **1c-1d** and MeI:

[$PtMe_2$I(ppy)(pz)], **2c**. ^{1}H NMR data: δ 1.28 [s, 3H, $^2J_{PtH}$ = 73.4 Hz, Me ligand *trans* to N atom of C^N ligand], 1.75 [s, 3H, $^2J_{PtH}$ = 69.2 Hz, Me ligand *trans* to I], 7.24–8.65 [11H, protons of C^N and pz ligand], 10.15 [m, 1H, $^3J_{PtH}$ = 10.1 Hz, CH group adjacent to coordinated N atom].

[$PtMe_2$I(ppy)(py)], **2d**. Yield: 81%, mp = 189 °C (decomp). Anal. Calcd. for $C_{18}H_{19}IN_2Pt$: C, 36.9; H, 3.3; N, 4.8; Found: C, 37.1; H, 3.2; N, 4.7.^{1}H NMR data: δ 1.19 [s, 3H, $^2J_{PtH}$ = 71.6 Hz, Me ligand *trans* to N atom of C^N ligand], 1.77 [s, 3H, $^2J_{PtH}$ = 69.5 Hz, Me ligand *trans* to py], 7.10–8.61 [12H, protons of C^N and py ligand], 10.17 [m, 1H, $^3J_{PtH}$ = 11.6 Hz, CH group adjacent to coordinated N atom].

2.3. Kinetic measurements

The kinetic rate constants were determined through UV–vis spectroscopy by monitoring the changes in absorbance. A linear relationship between absorbance, Abs, and concentration, *C*, confirmed the validity of the Beer–Lambert law ($Abs = \varepsilon bC$, b = path length = 1 cm) for all of the complexes. The kinetic measurements were monitored under *pseudo*-first-order conditions with [MeI] ≫ 10[Pt(II) complexes]. The concentrations of the Pt(II) complexes were 1.5×10^{-4} M. The *pseudo*-first-order rate constants, k_{obs}, were calculated by fitting the kinetic data to the first-order equation $Abs_t = Abs_\infty + (Abs_0 - Abs_\infty)\exp(-k_{obs}t)$, in which Abs_t = absorption at time t, Abs_0 = initial absorption, and Abs_∞ = infinity absorption. The experimentally determined *pseudo*-first- order rate constants were converted into second-order rate constants, k_2, by determining the slopes of the linear plots of k_{obs} against the concentration of MeI at the corresponding temperature according to the equation $k_{obs} = k_2$[MeI]. The activation parameters $\Delta H^{\ddagger}$ and $\Delta S^{\ddagger}$ for the reactions in acetone were obtained from kinetic experiments at five temperatures between 5 and 35 °C. The activation parameters were determined from the Eyring equation $\ln(k_2/T) = \ln(k_B/h) - \Delta H^{\ddagger}/RT + \Delta S^{\ddagger}/R$, in which $\Delta H^{\ddagger}$ = activation enthalpy, $\Delta S^{\ddagger}$ = activation entropy, k_2 = rate constant, k_B = Boltzmann constant, T = temperature, h = Planck constant, and R = universal gas constant.

2.4. Computational details

Gaussian 09 [22] was used for DFT calculations at the B3LYP [23,24] level of theory. The starting structures were created by GaussView program and optimized using the polarizable conductor

model (CPCM) continuum solvation methods [25] considering radii and acetone as solvent as implemented in Gaussian program. The effective core potential of Hay and Wadt with a double-ξ valence basis set (LANL2DZ) was chosen to describe Pt and I [26]. The 6-31G(d) basis set was used for other atoms [27]. Frequency calculations were carried out at the same level of theory. These calculations indicated the correct stationary points, characterized by the number of negative eigenvalues of their analytic Hessian matrix (0 for minima and 1 for any true transition state). We have also checked that imaginary frequencies exhibit the expected motion. All reported reaction and activation energies include zero-point energies and thermal corrections at 298 K and 1 atm. pressure to the electronic energies to allow direct comparison between theoretical and experimental data. To estimate the corresponding thermodynamic and activation parameters, we calculated the relevant corrections and added them to related energies.

3. Results and discussion

3.1. Synthesis and characterization of Pt complexes

Reaction of the dimethylsulfide complexes [PtMe(C^N)(SMe_2)], (C^N = bhq, **A**; C^N = ppy, **B**) with the nitrogen donor ligand L = pyrazine (pz) or pyridine (py) in an excess molar ratio gave the corresponding organoplatinum(II) complexes [PtMe(C^N)L], **1a**–**1d** (C^N = bhq, L = pz, **1a**; C^N = bhq, L = py, **1b**; C^N = ppy, L = pz, **1c**; C^N = ppy, L = py, **1d**). They were characterized by their ^{1}H NMR spectra and elemental analysis (for L = py). Complex **1d** was further characterized by x-ray crystallography (see Figure S1 and Table S1). These complexes were treated with excess methyl iodide in acetone or chloroform to give the corresponding six-coordinate cyclometalated Pt(IV) complexes [$PtMe_2$I(C^N)(L)], **2a**–**2d** (C^N = bhq, L = pz, **2a**; C^N = bhq, L = py, **2b**; C^N = ppy, L = pz, **2c**; C^N = ppy, L = py, **2d**) as shown in Scheme 1.

One may argue that N-methylation of the free N atom of pyrazine ligand in complexes **1a** and **1c** may compete with attacking of Pt(II) center on Me group of MeI reagent. Some systems [28] such as [$PtMe_2$(NN)], where NN = 2,2′-bipyrimidine or bis(2-pyridinal) ethylenediimine [29] and [PtMe(bpy-H)(PMe_3)] [30], has already been reported in the literature, each having at least one free N atom on the NN or C^N ligand, react with MeI to give the corresponding Pt(IV) products rather than N-methylation at free N atom. On the other hand, it is predicted [20] the rollover cyclometalated platinum(II) complexes [PtMe(C^N)(PPh_3)] (C^N = 2,3′-bpyridinate or 2,4′-bpyridinate) containing two potential nucleophilic centers, react with MeI through the free nitrogen donor to form N-methylated platinum(II) complexes rather than oxidative addition reaction to give Pt(IV) complexes. In the new pyrazine complexes **1a** and **1c**, the two competition reactions are suggested and shown in Scheme 1.

As an example, the reaction of complex **1a** with MeI was monitored by ^{1}H NMR and UV–Vis spectroscopies to find out which product is formed, **2a** (product of oxidative addition) or **3a** (product of N-methylation reaction), see Scheme 1. Typical ^{1}H NMR spectra for monitoring the reaction of **1a** with MeI in $CDCl_3$ at room temperature are shown in Fig. 1. Immediately after the addition of MeI, both species, that is, the Pt(II) complex and the Pt(IV) complex, can be observed in the first ^{1}H NMR spectrum. The signal for the Pt(II) complex (**1a**) disappears after a few minutes, and then the complex **2a** is gradually formed. As is clear from Fig. 1, the product of this reaction is the Pt(IV) complex **2a** instead of Pt(II) complex **3a** (see Scheme 1). In the ^{1}H NMR spectrum, for the product **2a**, two singlets with platinum satellites at $\delta = 1.20$ ($^2J_{PtH} = 73.5$ Hz) and $\delta = 1.84$ ($^2J_{PtH} = 69.5$ Hz) were assigned to the two different Me groups connected directly to Pt center. These $^2J_{PtH}$ values are rather smaller than that for Pt(II) complex **1a** ($^2J_{PtH} = 87.6$ Hz), confirming oxidation of Pt(II) complex **1a** to Pt(IV) complex **2a** (instead of formation of N-methylation product **3a**). A similar behavior was found for the reaction of ppy analogue complex **1c** with MeI.

To understand why the Pt center of complexes **1a** and **1c** can react with MeI instead of the free nitrogen donor of the pyrazine and to understand factors governing these two competing reactions (i.e. oxidative addition on Pt(II) *versus* N-methylation of coordinated pyrazine), we theoretically and experimentally studied the mechanism of both N-methylation and oxidative addition of the present reactions to examine and understand site selectivity. The suggested mechanisms are presented in Scheme 2.

3.2. DFT investigation of the reactions

First to predict the product of the reaction of complexes **1a** and **1c** with MeI, DFT calculations were used to investigate the mechanism of the reactions (Scheme 2). The structures of the starting complexes, suggested transition states, intermediates, and possible products were optimized by DFT calculations (see Supporting Information).

In the oxidative addition pathway, the nucleophilic attack of the $5d_{z^2}$ atomic orbital of the Pt(II) center of complex **1a** on the σ*-orbital of Me group of MeI (see Fig. 2) results in the formation of transition state **TSa** in which the Pt–C_{Me}–I angle is 176.8°, which indicates a linear structure with a planar Me ligand at the center (see Fig. 2 and Tables S2-S5). In this structure, the Me group is approaching the metal center, and the C–I bond is gradually breaking to form the cationic **IMa** intermediate, which has a distorted square-pyramidal geometry with incoming Me ligand located at the apical position. The completion of the oxidative

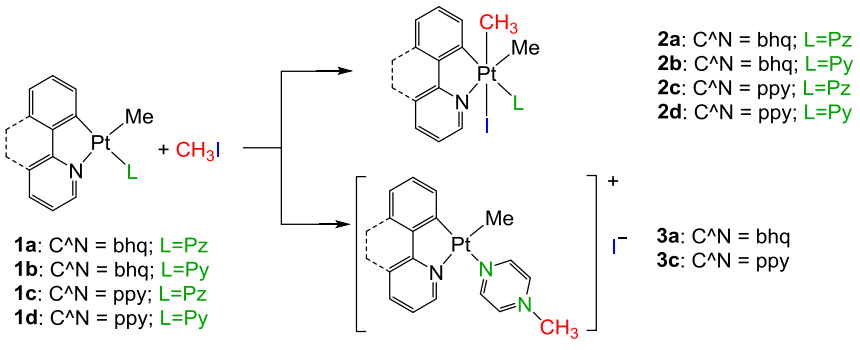

Scheme 1. Reactions studied in this work.

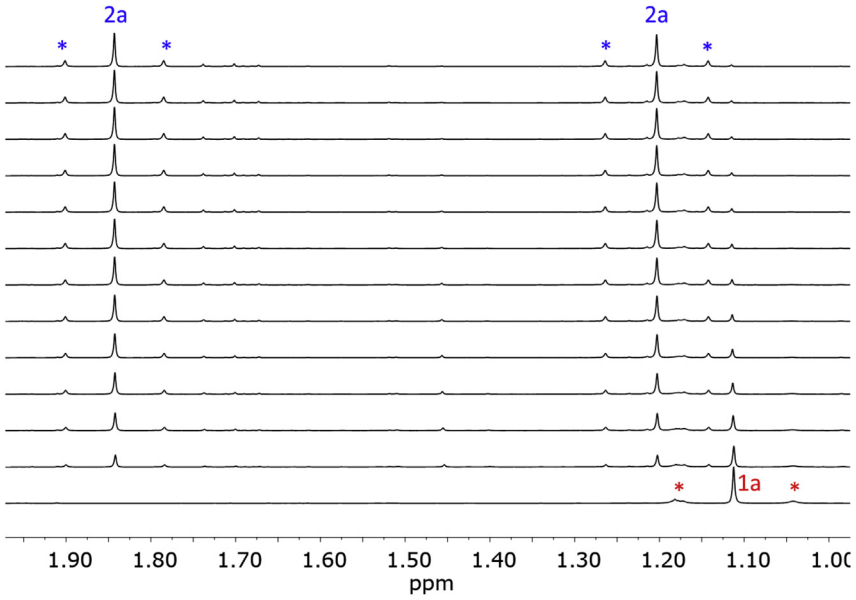

Fig. 1. Monitoring the addition of MeI to complex **1a** in $CDCl_3$ at room temperature by ^1H NMR spectroscopy (aliphatic region). The time interval is 3 min. Pt satellites are shown by asterisk.

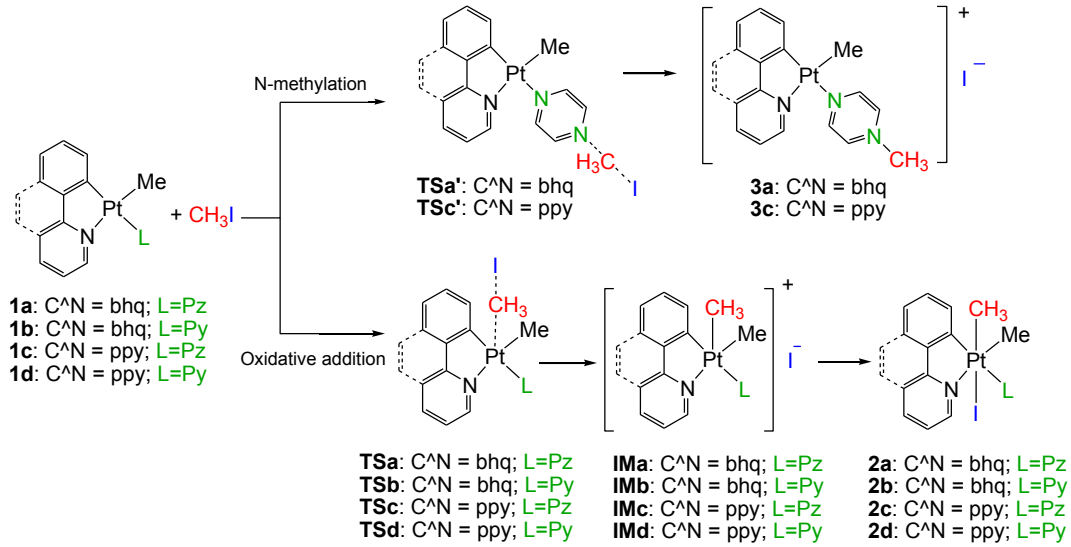

Scheme 2. Suggested mechanisms for N-methylation (top) and oxidative addition (bottom) reactions. Potential transition states and intermediates are shown.

addition then involves coordination of iodide anion to vacant site of **IMa** to give the product **2a**. In the N-methylation reaction, the free N atom of pyrazine attacks the CH_3 group of MeI. As shown in Scheme 2 and Fig. 2, transition state **TSa′** is formed. This transition state contains the linear arrangement of N–C_{Me}–I with bond angle of 179.4°. Similar to **TSa**, the coordination sphere around the C atom is trigonal bipyramid with N–C_{Me}–H bond angle of 89.1°. During the formation of **TSa′**, N–CH_3 and CH_3–I bond lengths vary significantly. The N–C_{MeI} length decreases from far apart in the reactants to 2.080 Å in the transition state, whereas the C–I length increases from 2.196 Å in MeI to 2.691 Å in transition state **TSa′**.

Fig. 3 shows the nature of the frontier molecular orbitals of the species involved in the oxidative addition reaction. For example, in the reaction of **1a** with MeI, the electronic configuration of the Pt(II) metal center is $d_{xz}^2 d_{yz}^2 d_{xy}^2 d_{z^2}^2 d_{x^2-y^2}^0$, with the d_{z^2} orbital being the HOMO-1. As shown in Fig. 3, the main contribution of Pt–C(MeI) in the HOMO of the transition state of **TSa** (oxidative addition reaction) comes from the overlap of the d_{z^2} of the platinum center with the LUMO of MeI (which is the C–I σ* antibonding molecular orbital). So the oxidation process can be considered as the removal of electrons from the HOMO-1 of the complex [PtMe(bhq)(pz)] into the LUMO of MeI. Similar result was observed for the N-methylation reaction of MeI with free N atom of pyrazine in complex **1a**, where C–I σ* antibonding MO overlaps with N atom to locate the electron density on I atom of **TSa′**. As is clear from Fig. 3, the electron density in **1a** is more located on the Pt atom instead of N free atom of pyrazine which enables the Pt center to act as a stronger nucleophile than N free donor towards MeI.

Qualitative representations of the highest occupied and lowest unoccupied molecular orbitals in [PtMe(bhq)(pz)], **1a**, [$PtMe_2$I(bhq)(pz)], **2a**, and [PtMe(bhq)(pz-Me)]I, **3a**, are presented in Fig. 4. The HOMO–LUMO gap of **1a** is equal to 3.034 eV. HOMO

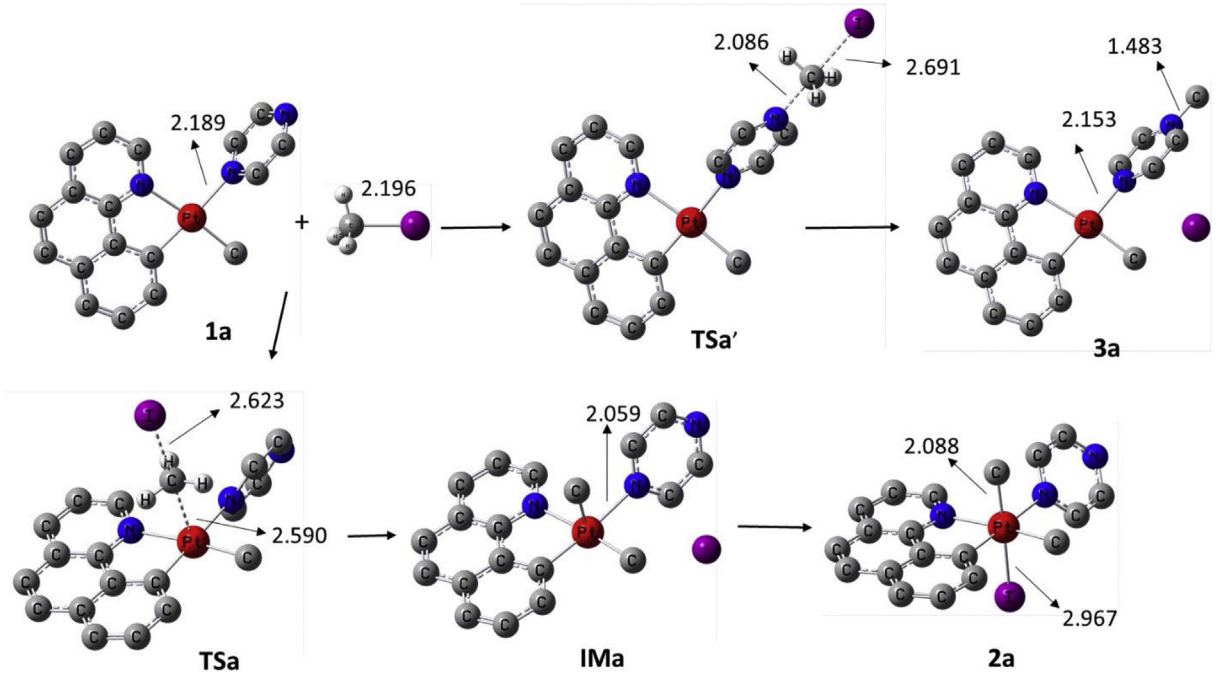

Fig. 2. Structural change in oxidative addition and N-methylation of complex **1a** and the optimizes geometries in acetone solvent. Bond lengths and angles are in Å and °, respectively. H atoms (except for moving Me) are removed for more clarity.

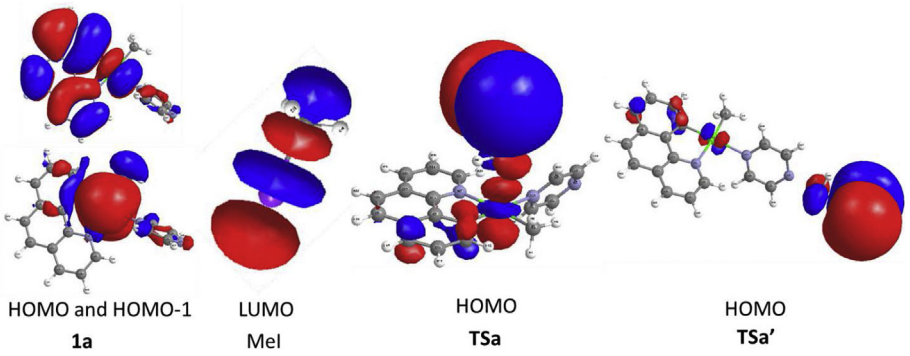

Fig. 3. Selected frontier orbitals in acetone solvent; HOMO and HOMO-1 of complex **1a**; LUMO of MeI; HOMO of **TSa** and HOMO of **TSa′**.

and HOMO-1 of **1a** consist mainly the Pt *d* orbital and bhq ligand orbitals. The LUMO is predominately localized on the pyrazine ligand orbitals. The value of the energy separations between the HOMO and LUMO of **2a** and **3a** are smaller than that of **1a** and are equal to 2.910 and 1.121 eV, respectively. The HOMO and HOMO-1 of Pt(IV) complex **2a** are mostly located on I atom and the LUMO of this complex is mainly localized on the pyrazine ligand. The HOMO and LUMO of **3a** can also be ascribed as a combination of Pt atom, pz and bhq ligands, where the contribution of bhq ligand in HOMO is more than that in LUMO (see Fig. 4).

To predict the product of the reaction of complexes **1** with MeI, DFT calculations were used to obtain the energies of species involved in the oxidative addition and N-methylation reactions. The DFT calculated data for the reactions shown in Scheme 2 in acetone are collected in Table 1.

The calculated energy profile for the oxidative addition and N-methylation reactions of **1a** with MeI is shown in Fig. 5. Furthermore, all of the optimized structures with selected geometric parameters are shown in Tables S2–S5. The summation of the free energies of the Pt(II) complex and MeI was considered to be zero, and the other energy levels vary relative to this (Fig. 5). As shown in Fig. 5, the energy barriers ($\Delta G^{\ddagger}$ in kcalmol^{-1}, see Table 1) for the oxidative addition and N-methylation reactions of complex **1a** with MeI in acetone are 79.4 and 101.6 kJmol^{-1}, respectively, which shows the lower energy barrier for oxidative addition reaction. This behavior can also predict from the shape of highest occupied molecular orbitals of **1a** (see Fig. 3) where the electron density is more concentrated on the Pt atom comparing to free N atom of pyrazine which enables the former to be stronger nucleophile than free N donor towards MeI. This observation is consistent with the experimental finding in which the Pt(IV) complex **2a** (and not **3a**, see Scheme 1) is the product of the reaction of complex **1a** with MeI. In the energy profiles, the calculated energy barrier for oxidative addition reaction of complex **1a** with MeI, as the energy gaps between the starting materials and the transition state **TSa**, has also a good agreement with the $\Delta G^{\ddagger}$ values obtained from the kinetic experiment (73.6 kJmol^{-1}, see the experimental results summarized in Table 2). One possible interpretation for higher energy barrier observed for the N-methylation reaction with respect to oxidative addition is the coordination of Pt(II) center to nitrogen

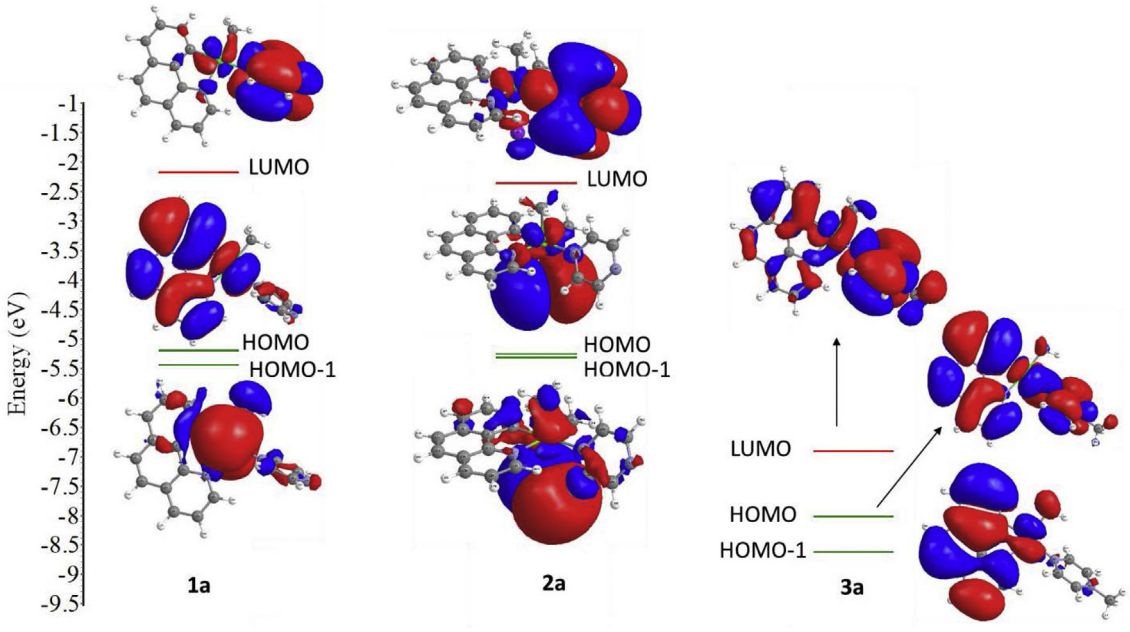

Fig. 4. Qualitative frontier molecular orbitals scheme for complexes **1a**, **2a** and **3a**.

Table 1
Computed activation parameters and reaction thermodynamics for oxidative addition and N-methylation reactions shown in Scheme 2.

	$\Delta H^{\ddagger}$ kJ/mol	$\Delta S^{\ddagger}$ J/mol K	$\Delta G^{\ddagger}$ kJ/mol	ΔH° kJ/mol	ΔS° J/mol K	ΔG° kJ/mol
N-methylation						
1a	59.0	−142.6	101.6	−17.7	−55.9	−1.0
1c	59.3	−137.7	100.4	−17.8	−57.0	−0.8
1e[a]	61.5	−141.5	103.6	−13.2	−56.2	3.6
Oxidative addition						
1a	35.6	−147.5	79.4	−49.6	−172.9	1.9
1b	33.4	−149.4	77.9	−51.7	−175.6	0.7
1c	35.8	−142.6	79.3	−49.5	−177.8	3.5
1d	34.7	−144.4	77.7	−51.4	−179.7	2.1
1e[a]	35.5	−146.9	79.3	−50.7	−173.9	1.2

[a] L = pyrimidine.

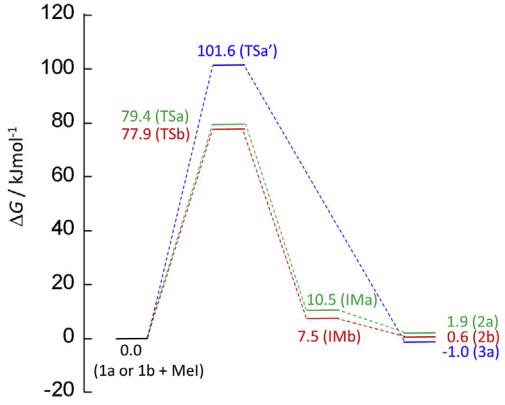

Fig. 5. Calculated relative free energies for products, intermediates and transition states, arising from the oxidative addition (green) and N-methylation (blue) of complex **1a** and oxidative addition of complex **1b** (red) by MeI in acetone. The summation of the energies of the **1a** or **1b** and MeI was considered to be zero. (For interpretation of the references to colour in this figure legend, the reader is referred to the Web version of this article.)

atom of pyrazine which appears to reduce the nucleophilicity of the remaining nitrogen-donor such that the Pt(II) center of **1a** is a stronger nucleophile than the free pyrazine nitrogen donor.

As shown in Fig. 5, the free energy barrier for oxidative addition reaction of pyridine complexes (for example 77.9 kJmol^{-1} for complex **1b**) is slightly less than that for pyrazine complexes (for example 79.4 kJmol^{-1} for complex **1a**). This may be due to the influence of extra nitrogen atom of pyrazine ligand. The extra electronegative nitrogen atom in pyrazine ligand makes this ligand slightly weaker donor than pyridine, thus decreasing the electron density of Pt(II) in the complex and therefore the reaction rate of [PtMe(C^N)(pz)] compared to [PtMe(C^N)(py)], as supported by experimental findings (see next section).

We extended our DFT calculation to other ligand, pyrimidine (see 1e, Scheme 3) to find out the position effect of extra N atom in N donor ligand on the possibility of N-methylation versus oxidative addition (see Table 1). As can be seen in Table 1, the free energy barrier for MeI oxidative addition on Pt(II) center is almost the same as that found for complex **1a** (79.4 and 79.3 kJmol^{-1} for **1a** and **1e**, respectively) due to identical nucleophilicity of Pt centers in these complexes and are lower than those calculated for N-methylation (101.6 and 103.6 kJmol^{-1} for **1a** and **1e**, respectively).

We have previously reported the theoretical investigation of N-methylation versus oxidative addition of rollover cyclo-platinated(II) complexes [PtMe(2,X′-bpy-H)(PPh$_3$)], (X = 2, **F**; X = 3, **G**; and X = 4, **H**) by MeI (see Scheme 3) [20]. We found that though complex **F** reacts with MeI through oxidative addition reaction to give Pt(IV), the analogous complexes **G** and **H** are predicted to attend in N-methylation. This different behavior was attributed to the position of the nitrogen atom in the bpy-H ligand in which steric hindrance prohibits N-methylation in complex **F**, while its absence on the free N atom in complexes **G** and **H** favors N-methylation. Although in that case steric effect around free N atom has an important role, in the case of pyrazine complex **1a** presence of an extra nitrogen atom may reduce the nucleophilicity of the remaining nitrogen-donor and favor oxidative addition over N-methylation.

Table 2
Second-order rate constants[a] and activation parameters for the reactions of complexes **1** with MeI in acetone.

Complex	λ_{max} /nm	10^2k_2/Lmol^{-1}s^{-1} at different temperatures (°C)							$\Delta H^{\ddagger}$ /kJmol^{-1}	$\Delta S^{\ddagger}$ /Jmol^{-1}K^{-1}	$\Delta G^{\ddagger}$ /kJmol^{-1}
		5	10	15	20	25	30	35			
1a	395	0.27	0.34	–	0.56	0.81	0.95	–	33.6 ± 1.8	−134 ± 6	73.6 ± 2.5
1b	395	0.81	1.01	1.19	–	1.8	–	2.9	27.4 ± 1.3	−147 ± 4	71.2 ± 1.8
1c	370	0.29	0.38	–	0.65	0.81	1.02	–	32.9 ± 0.5	−136 ± 1	73.4 ± 0.6
1d	370	0.79	1.07	1.31	–	2.2	–	3.21	30.7 ± 0.9	−135 ± 3	71.0 ± 1.3

[a] Estimated errors are ±5%.

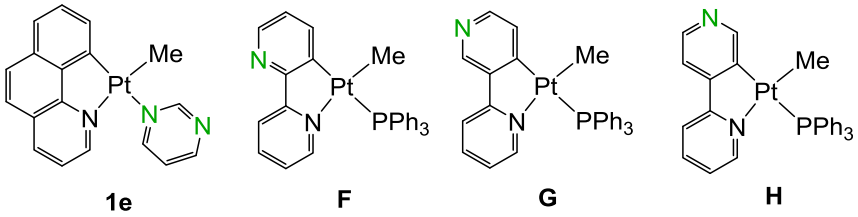

Scheme 3. Structure of complexes **1e**, **F**, **G** and **H**.

3.3. Kinetic and mechanism of the reaction of complexes *1a-1d* with MeI

As stated in the last section, DFT calculations predict that complexes **1a** and **1c** (where C^N = pz) react with MeI through the Pt center to form Pt(IV) complex. To find out the accuracy of our prediction from DFT calculations, the oxidative addition reactions of **1a** and **1c** with MeI in acetone were experimentally studied. The complexes **1** have $5d_{\pi}(Pt) \rightarrow \pi^*$ (C^N) metal-to-ligand charge-transfer bands in the visible region, which were used to easily follow the kinetics of their reactions with MeI by monitoring the disappearance of the MLCT band of the Pt(II) complexes. The *pseudo*-first-order rate constants k_{obs} were obtained by nonlinear least-squares fitting of the absorbance–time curves to a first-order equation $Abs_t = Abs_{\infty} + (Abs_0 - Abs_{\infty}) \exp(-k_{obs}t)$. The k_{obs} values were plotted against [MeI] at different temperatures. They displayed good straight-line plots and the slope of each line gave the second-order rate constant (k_2). Typical changes in the UV–Vis spectrum of complex **1a** at room temperature and plots of k_{obs} versus the [MeI] at different temperatures during the reaction of **1a** with MeI in acetone solution are shown in Fig. 6. The Eyring equation is also used to calculate the activation parameters (see Fig. 7) and the resulting kinetic data are summarized in Table 2.

On the basis of the kinetic data, we suggest that (see Scheme 2, bottom) Pt(II) center of each of the complexes **1**, first attacks as a nucleophile on the carbon atom of MeI to give an ionic five-coordinate intermediate $[PtMe_2(C^N)(L)]^+I^-$ with a square pyramidal geometry having the incoming Me in the apical position and the iodide ion in the outer sphere of the Pt complex. Then the free iodide ion coordinates to Pt(IV) center of the $[PtMe_2(C^N)(L)]^+$ intermediate to form the octahedral Pt(IV) product $[PtMe_2I(C^N)(L)]$, **2**.

In a comparative study, we studied the kinetics of reaction of pyridine analogues [PtMe(C^N)(py)], (C^N = bhq, **1b**; C^N = ppy, **1d**), with MeI as a "calibration reaction" to evaluate the reality of kinetic data obtained for pyrazine complexes and the effect of N-donor ligand on the rate of the reaction of MeI with complexes **1**. The Pt(II) complexes **1b** and **1d** also contain a MLCT band in the visible region and was used similarly to study the kinetics of their reactions in acetone at $\lambda = 395$ and 370 nm for **1b** and **1d**, respectively. The data are collected in Table 2. As clear from Table 2, the activation parameters obtained for pyridine complexes **1b** and **1d** (which attend

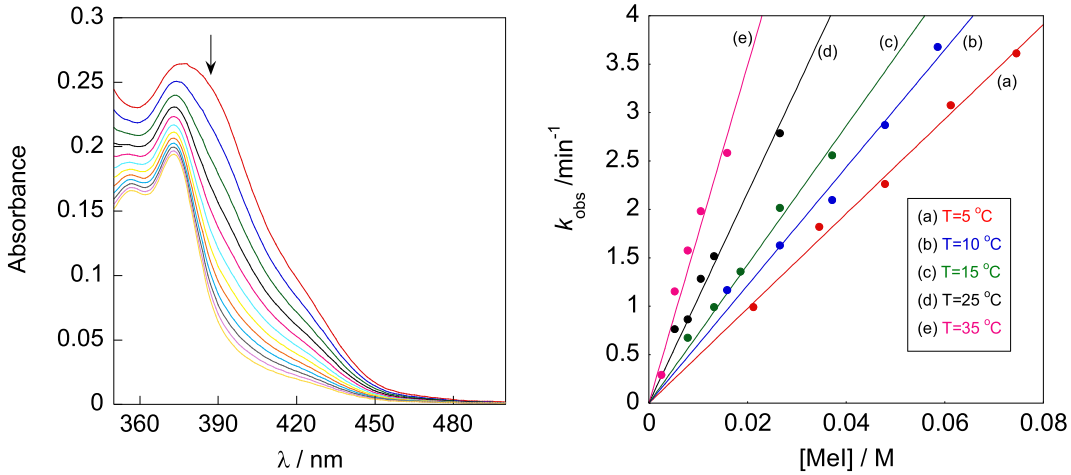

Figure 6. (Left) Changes in the UV–Vis spectrum of **1a** with MeI in acetone at 25 °C; (Right) the plots of *pseudo*-first-order rate constants (k_{obs}/min^{-1}) versus [MeI] for the reaction of **1b** with MeI in acetone at different temperatures.

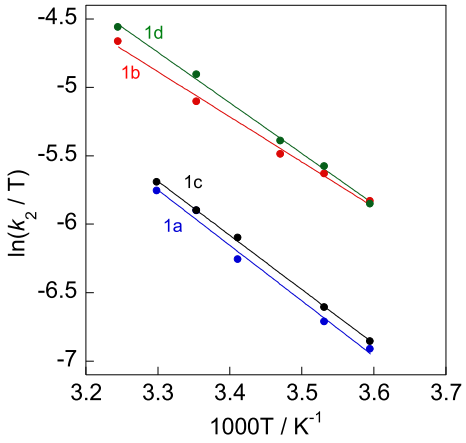

Fig. 7. Eyring plots for reaction of the complexes **1a**-**1d** with MeI in acetone.

only in the oxidative addition reaction instead of N-methylation) are in the range of those observed for pyrazine complexes (**1a** and **1c**). This may be taken as an evidence for operation of a common mechanism (S_N2) in this series of oxidative addition reactions.

As reported in Table 2, for the pyridine derivatives (**1b** and **1d**) the rate constants are almost 3 fold those for the pyrazine derivatives, matching with that expected on electronic grounds. The extra electronegative nitrogen atom in pyrazine makes this ligand weaker donor, thus decreasing the negative-charge density at the Pt(II) center and therefore decreasing the reaction rates for complexes **1a** and **1c** compared to **1b** and **1d**. The rate constants observed for bhq complexes (**1a** and **1b**) or their ppy analogues (**1c** and **1d**) are almost the same showing that both C^N ligands have the same donor ability on Pt(II) centers. For example, the rate constants for reactions of complexes **1a** and **1c** with MeI at 25 °C are 0.81 $Lmol^{-1}s^{-1}$.

It should be noted that our experimental findings strongly support DFT calculations. The trend for the experimental values of free energy barriers of oxidative addition reactions [**1a** (73.6 $kJmol^{-1}$) ≅ **1c** (73.4 $kJmol^{-1}$) > **1b** (71.2 $kJmol^{-1}$) ≅ **1d** (71.0 $kJmol^{-1}$)] reflects the observed trend for the calculated $\Delta G^{\ddagger}$ values (79.4, 79.3 77.9 and 77.7 $kJmol^{-1}$ for **1a**, **1c**, **1b** and **1d**, respectively, see Table 1).

4. Conclusions

New cycloplatinated(II) complexes of the general formula [PtMe(C^N)(pz)], (C^N = bhq, **1a**; C^N-ppy, **1c**) have two potentially nucleophilic sites for reaction with MeI, a Pt(II) center (to undergo oxidative addition) and the N atom of pyrazine ligand (to undergo N-methylation). Theoretical calculations predict that these complexes would favor oxidative addition with MeI to give Pt(IV) products. The energy barriers ($\Delta G^{\ddagger}$) for N-methylation of complexes **1a** and **1c** are 101.6 and 100.3 kJ mol^{-1}, respectively, which are much higher than those for oxidative addition, 79.4 and 77.9 kJ mol^{-1}, respectively. The calculated reaction profiles were confirmed experimentally, in which the oxidation of Pt(II) to Pt(IV) complexes is clearly demonstrated by ^1H NMR. Furthermore, the kinetics studies using UV–vis spectroscopy indicate that MeI reacts with the Pt(II) center of [PtMe(C^N)(pz)], (**1a** or **1c**), with a rate significantly lower than that of the corresponding reaction involving [PtMe(C^N)(py)], **1b** or **1d**, which was studied as a "reference reaction". This observation has been attributed to more electron donating ability of pyridine in complex **1b** (or **1d**) compared to pyrazine in complex **1a** (or **1c**) because of the presence of an extra electronegative nitrogen atom in the pyrazine ligand. It should be noted that the free energy barriers for oxidative addition of complexes **1a** (C^N = bhq) and **1c** (C^N = ppy) (79.4, and 79.3 k $Jmol^{-1}$, respectively) are comparable, showing that the Pt centers in these complexes have similar nucleophilicity; and these experimental value are in excellent agreement with those obtained from computations of transition-states by DFT.

Acknowledgments

F.N.H. acknowledges the support of the Islamic Azad University, Shiraz Branch, for her sabbatical leave at University of California, Santa Barbara. We acknowledge support from the Center for Scientific Computing from the CNSI, MRL: an NSF MRSEC (DMR-1121053) and NSF CNS-0960316, and support from the Shiraz University and the Department of Chemistry and Biochemistry at UCSB.

Appendix A. Supplementary data

Supplementary data to this article can be found online at https://doi.org/10.1016/j.jorganchem.2018.11.002.

References

[1] A. Armstrong, Modern Amination Methods by a. Ricci. Wiley-vch, ACS Publications, Weinheim, 2000, p. 2001.
[2] Z. Rappoport, The Chemistry of Anilines, John Wiley & Sons, 2007.
[3] H.K. Santhapuram, A. Datta, O.E. Hutt, G.I. Georg, N-Methylation of the C3′ amide of taxanes: synthesis of N-methyltaxol C and N-methylpaclitaxel, J. Org. Chem. 73 (2008) 4705–4708.
[4] P. Tundo, M. Selva, The chemistry of dimethyl carbonate, Acc. Chem. Res. 35 (2002) 706–716.
[5] Y. Li, I. Sorribes, T. Yan, K. Junge, M. Beller, Selective methylation of amines with carbon dioxide and H_2, Angew. Chem. Int. Ed. 52 (2013) 12156–12160.
[6] K. Beydoun, T. vom Stein, J. Klankermayer, W. Leitner, Ruthenium-catalyzed direct methylation of primary and secondary aromatic amines using carbon dioxide and molecular hydrogen, Angew. Chem. Int. Ed. 52 (2013) 9554–9557.
[7] X. Cui, X. Dai, Y. Zhang, Y. Deng, F. Shi, Methylation of amines, nitrobenzenes and aromatic nitriles with carbon dioxide and molecular hydrogen, Chem. Sci. 5 (2014) 649–655.
[8] C.E. Hickey, P.M. Maitlis, Oxidative addition of methyl Iodide to dicarbonylrhodium (I) complexes, J. Chem. Soc. Chem. Commun. (1984) 1609–1611.
[9] P.B. Chock, J. Halpern, Kinetics of the addition of hydrogen, oxygen, and methyl iodide to some square-planar iridium(I) complexes, J. Am. Chem. Soc. 88 (1966) 3511–3514.
[10] P.J. Stang, M.D. Schiavelli, H.K. Chenault, J.L. Breidegam, Kinetic deuterium isotope effects in the reaction of Vaska's compound $(Ph_3P)_2Ir(CO)Cl$ with methyl iodide and $MeOSO_2CF_3$, Organometallics 3 (1984) 1133–1134.
[11] P. Hamidizadeh, M. Rashidi, S.M. Nabavizadeh, M. Samaniyan, M.D. Aseman, A.M. Owczarzak, M. Kubicki, Secondary kinetic deuterium isotope effect in oxidative addition reaction of cycloplatinated (II) complexes with MeI, J. Organomet. Chem. 791 (2015) 258–265.
[12] M.D. Aseman, M. Rashidi, S.M. Nabavizadeh, R.J. Puddephatt, Secondary kinetic isotope effects in oxidative addition of benzyl bromide to dimethylplatinum (II) complexes, Organometallics 32 (2013) 2593–2598.
[13] S. Habibzadeh, M. Rashidi, S.M. Nabavizadeh, L. Mahmoodi, F.N. Hosseini, R.J. Puddephatt, Steric and solvent effects on the secondary kinetic α-deuterium isotope effects in the reaction of methyl iodide with organoplatinum (II) complexes: application of a second-order technique in measuring the rates of rapid processes, Organometallics 29 (2009) 82–88.
[14] M. Crespo, M. Martinez, S.M. Nabavizadeh, M. Rashidi, Kinetico-mechanistic studies on CX (X= H, F, Cl, Br, I) bond activation reactions on organoplatinum (II) complexes, Coord. Chem. Rev. 279 (2014) 115–140.
[15] M.D. Aseman, S.M. Nabavizadeh, F. Niroomand Hosseini, G. Wu, M.M. Abu-Omar, Carbon–oxygen bond forming reductive elimination from cycloplatinated(IV) complexes, Organometallics 37 (2018) 87–98.
[16] S.M. Nabavizadeh, H. Amini, F. Jame, S. Khosraviolya, H.R. Shahsavari, F.N. Hosseini, M. Rashidi, Oxidative addition of MeI to some cyclometalated organoplatinum (II) complexes: kinetics and mechanism, J. Organomet. Chem. 698 (2012) 53–61.
[17] M. Zanganeh, S.J. Hoseini, M. Rashidi, S.M. Nabavizadeh, M.R. Halvagar, Reaction of allyl bromide with cyclometallated platinum (II) complexes: unusual kinetic behavior and a novel case of methyl and allyl CC bond reductive elimination, J. Organomet. Chem. 856 (2018) 1–12.
[18] H.R. Shahsavari, R. Babadi Aghakhanpour, M. Babaghasabha, M. Golbon Haghighi, S.M. Nabavizadeh, B. Notash, Combined kinetico-mechanistic and

theoretical elucidation of the oxidative addition of iodomethane to cycloplatinated(II) complexes: controlling the rate of trans/cis isomerization, Eur. J. Inorg. Chem. (2017) 2682–2690, 2017.
[19] K.R. Pichaandi, L. Kabalan, H. Amini, G. Zhang, H. Zhu, H.I. Kenttämaa, P.E. Fanwick, J.T. Miller, S. Kais, S.M. Nabavizadeh, M. Rashidi, M.M. Abu-Omar, Mechanism of Me–Re bond addition to platinum (II) and dioxygen activation by the resulting Pt–Re bimetallic center, Inorg. Chem. 56 (2017) 2145–2152.
[20] F. Niroomand Hosseini, S.M. Nabavizadeh, M.M. Abu-Omar, Which is the stronger nucleophile, platinum or nitrogen in rollover cycloplatinated (II) complexes? Inorg. Chem. 56 (2017) 14706–14713.
[21] M.G. Haghighi, S.M. Nabavizadeh, M. Rashidi, M. Kubicki, Selectivity in metal–carbon bond protonolysis in p-tolyl-(or methyl)-cycloplatinated (II) complexes: kinetics and mechanism of the uncatalyzed isomerization of the resulting Pt (II) products, Dalton Trans. 42 (2013) 13369–13380.
[22] M. Frisch, G. Trucks, H. Schlegel, G. Scuseria, M. Robb, J. Cheeseman, G. Scalmani, V. Barone, B. Mennucci, G. Petersson, Gaussian 09, Revision D. 01, Gaussian, Inc., Wallingford CT, 2009.
[23] P. Stephens, F. Devlin, C. Chabalowski, M.J. Frisch, Ab initio calculation of vibrational absorption and circular dichroism spectra using density functional force fields, J. Phys. Chem. 98 (1994) 11623–11627.
[24] R.G. Parr, W. Yang, Density-functional theory of the electronic structure of molecules, Annu. Rev. Phys. Chem. 46 (1995) 701–728.
[25] M. Cossi, N. Rega, G. Scalmani, V. Barone, Energies, structures, and electronic properties of molecules in solution with the C-PCM solvation model, J. Comput. Chem. 24 (2003) 669–681.
[26] P.J. Hay, W.R. Wadt, Ab initio effective core potentials for molecular calculations. Potentials for the transition metal atoms Sc to Hg, J. Chem. Phys. 82 (1985) 270–283.
[27] P.C. Hariharan, J.A. Pople, The influence of polarization functions on molecular orbital hydrogenation energies, Theor. Chim. Acta 28 (1973) 213–222.
[28] M.S. McCready, R.J. Puddephatt, The platinum center is a stronger nucleophile than the free nitrogen donors in a dimethylplatinum complex with a dipyridylpyridazine Ligand, Organometallics 34 (2014) 2261–2270.
[29] J.D. Scott, R.J. Puddephatt, Comparison of the reactivities toward oxidative addition of the dimethylplatinum (II) units in mononuclear and binuclear complexes with bis (diimine) ligands, Organometallics 5 (1986) 2522–2529.
[30] R.B. Aghakhanpour, S.M. Nabavizadeh, L. Mohammadi, S.A. Jahromi, M. Rashidi, A kinetic approach to carbon–iodide bond activation by rollover cycloplatinated (II) complexes containing monodentate phosphine ligands, J. Organomet. Chem. 781 (2015) 47–52.